iScience

CellPress
OPEN ACCESS

Article

High-dimensional encoding of movement by single neurons in basal ganglia output

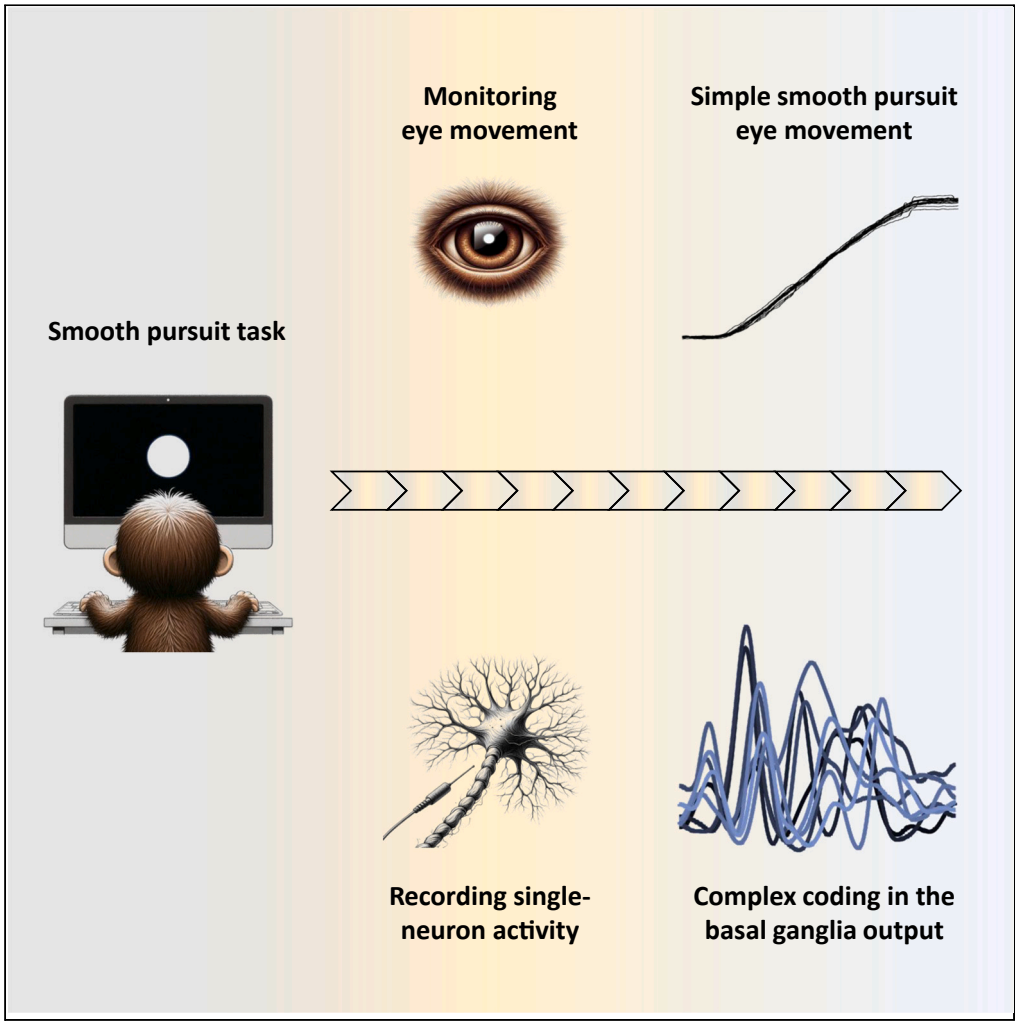

Gil Zur, Noga Larry, Matan Cain, Adi Lixenberg, Merav Yarkoni, Stuart Behling, Mati Joshua

gil.zur1@mail.huji.ac.il

Highlights

SNpr responses are more diverse than other cortical and subcortical populations

The diversity of responses depends on sensorimotor parameters

The diversity of responses to rewards varies as a function of different task epochs

Single neurons in the SNpr exhibit multidimensional responses

Zur et al., iScience *27*, 110667
September 20, 2024
https://doi.org/10.1016/j.isci.2024.110667

iScience

CellPress
OPEN ACCESS

Article

High-dimensional encoding of movement by single neurons in basal ganglia output

Gil Zur,[1,3,4,*] Noga Larry,[1,3] Matan Cain,[1] Adi Lixenberg,[1] Merav Yarkoni,[1] Stuart Behling,[2] and Mati Joshua[1]

SUMMARY

The substantia nigra pars reticulata (SNpr), an output structure of the basal ganglia, is hypothesized to gate movement execution. Previous studies in the eye movement system focusing mostly on saccades have reported that SNpr neurons are tonically active and either pause or increase their firing during movements, consistent with the gating role. We recorded activity in the SNpr of two monkeys during smooth pursuit and saccadic eye movements. SNpr neurons exhibited highly diverse reaction patterns during pursuit, including frequent increases and decreases in firing rate, uncorrelated responses in different movement directions and in reward conditions that resulted in the high dimensional activity of single neurons. These diverse temporal patterns surpassed those in other oculomotor areas in the medial-temporal cortex, frontal cortex, basal ganglia, and cerebellum. These findings suggest that temporal properties of the responses enrich the coding capacity of the basal ganglia output beyond gating or permitting movement.

INTRODUCTION

The basal ganglia are embedded within cortical and sub-cortical networks that drive movement.[1] Initial studies proposed that the basal ganglia directly controls behavior, with tonic inhibition limiting movement and pauses in basal ganglia activity facilitating movement.[2,3] However, rather than a binary coding of movement, studies showed that the output of the basal ganglia codes behavioral events by both increases and decreases in activity.[4,5] One explanation was that this pattern of activity might reflect the pattern of inhibition and excitation (disinhibition) required to drive movement.[6,7] Alternatively, the complexity of single neurons might not conform directly to movement parameters since complexity could emerge from internal computations, such as those found in the implementation of a dynamical system.[8,9] Complex temporal patterns of responses of single neurons that are not directly related to movement parameters are a signature of these dynamics. This raised the critical question in basal ganglia research of whether the temporal patterns of activity are complex, and how they are related to movement parameters.

The current study approached this issue by exploring the temporal patterns of the activity of single neurons in the basal ganglia during behavior. We focused on the eye movement system since it provides exquisite control over behavior, which has led to an extensive in-depth characterization of responses in the motor pathways.[10–12] These offer a framework for interpreting the observed temporal activity patterns. Previous research has mostly studied basal ganglia activity during saccadic eye movements.[5,13,14] However, the rapidity of saccades constrains the ability to identify temporal modulations in movement coding. In contrast, smooth pursuit eye movements are continuous and prolonged, which provides an opportunity to examine modulations that may be indiscernible during saccades.[10] To examine potential temporal modulations in movement coding, we recorded from the basal ganglia during both saccadic and pursuit eye movements.

Specifically, we recorded activity in the substantia nigra pars reticulata (SNpr), the basal ganglia output structure that is involved in both pursuit and saccade eye movements.[15,16] Single neural activity in the SNpr exhibits diverse temporal response patterns. These manifested in weak correlations between responses and the high dimensionality of single-neuron activity across directions of pursuit eye movements. In particular, the diversity of activity patterns was greater in the SNpr than in other oculomotor brain areas, including the caudate, cerebellum, medial-temporal cortex (MT), and frontal eye field. These findings underscore the importance of temporal coding in the basal ganglia output. The contrast between complex temporal patterns and simple pursuit behavior suggests that the basal ganglia do not merely encode basic parameters of behavior, such as gating movement or movement kinematics, but rather engage in intricate computational processes.

[1]Edmond and Lily Safra Center for Brain Sciences, the Hebrew University, Jerusalem, Israel
[2]Department of Neurobiology, Duke University School of Medicine, Durham, NC, United States
[3]These authors contributed equally
[4]Lead contact
*Correspondence: gil.zur1@mail.huji.ac.il
https://doi.org/10.1016/j.isci.2024.110667

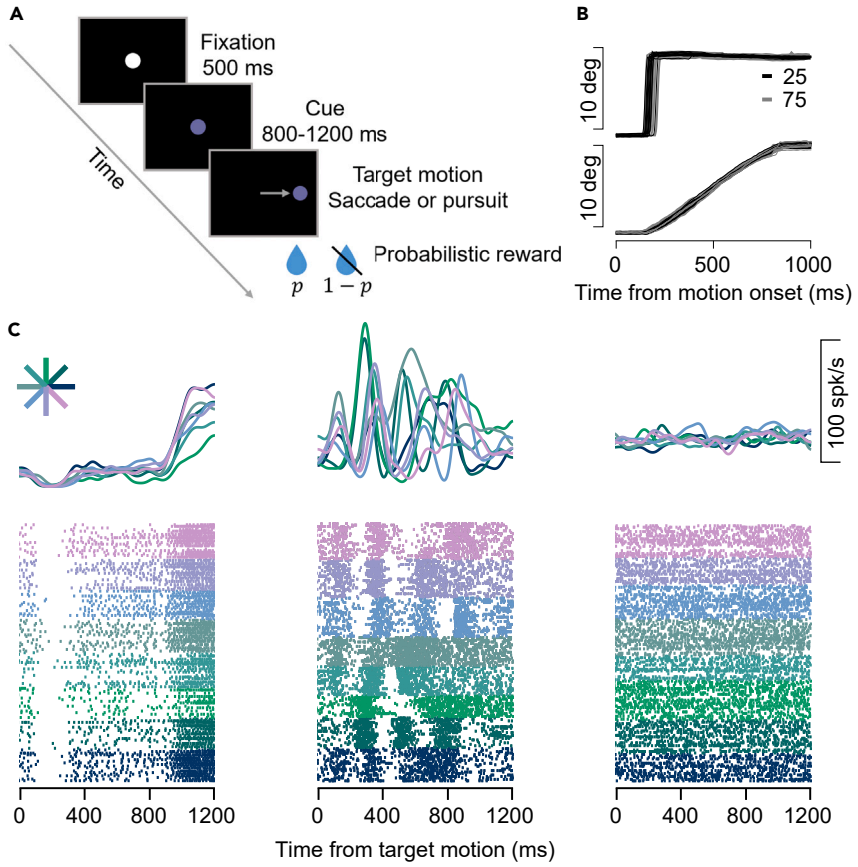

Figure 1. Behavioral task and example neurons

(A) Schematics of the task stages as they appeared on the screen: fixation target, color switch to cue reward probability, and target motion in one out of eight directions. A reward was delivered after completing the trial according to the probability (p) associated with the cue.

(B) Horizontal eye position for several saccades (top) and pursuit (bottom) trials in which the target moved to the right. The horizontal and vertical axis represent the time from motion onset and the eye position in degrees. The colors indicate the probability of receiving the reward.

(C) PSTH (top) and raster (bottom) of three example neurons. Each column shows a single neuron during target motion in a pursuit session. Colors indicate the direction of the target motion and correspond to the direction presented in the asterisk at the top of C.

RESULTS

Behavioral task and neural recordings

Two monkeys were trained on saccade and pursuit tasks in which we manipulated the reward probability (Figure 1A). Both tasks were initiated by a fixation stage in which a white fixation target appeared in the center of a black screen. After 500 ms, the target changed to one of two colors, indicating the probability of the reward given after the successful completion of the trial. One color corresponded to a probability of 75% and the other to a probability of 25%. After a random period (800–1200 ms) the target moved in one of eight directions. In the saccade task, the target instantaneously jumped to a 10° eccentric position. In the pursuit task, the target moved continuously at a speed of 20°/s.[17] The monkeys were required to track the target accurately to complete the trial. At the end of a successful trial, the monkeys received the reward corresponding to the probability specified by the color of the target. Figure 1B presents examples of horizontal eye positions on trials where the target moved to the right. In the saccade task, the monkeys saccades rapidly to the new location of the target, whereas on the pursuit task the monkeys followed the target smoothly until it stopped.

We recorded from the monkeys' SNpr (see Table 1) while they performed the eye movement tasks. Figure 1C shows the averages and trial-by-trial activity of example SNpr neurons recorded during the pursuit task. Since the effect of reward on behavior and neural activity during movement (but not the cue) was very small,[18] we initially grouped trials in two reward probability conditions based on the direction of movement. Later we address the effects of the reward probability in detail. The first neuron consistently paused its activity after the initiation of movement in all directions and trials (Figure 1C left). This pattern of activity is similar to findings elsewhere indicating that tonically active SNpr neurons exhibit either a pause or an increase during eye movements.[14–16] The second type of activity was characterized by a diverse reaction pattern across directions of movement (Figure 1C middle). Importantly, examination of the raster indicated that these multiphasic increases and decreases in firing rate were consistent across trials having the same direction of movement. By contrast, a neuron that did not

Table 1. Number of neurons analyzed in each task and area of recordings

Monkey	Task	SNpr	Striatum	Vermis	FEF	Flocculus	MT
Al	Pursuit	62	87	102			
	Saccade	38	63	66			
B	Pursuit					150	
C	Pursuit					117	
G	Pursuit	104	75	75			
	Saccade	115	108	89			
F	Pursuit				326		
	Saccade				260		
Ar	Pursuit						92
Di	Pursuit						111

respond to the task (Figure 1C right) was characterized by an inconsistent modulation between different trials, resulting in low average amplitude activity in the PSTH. Thus, these examples demonstrate that in our dataset, some neurons responded stereotypically as reported previously, whereas others exhibited diverse temporal patterns across directions of movement.

Characterizing the diversity of temporal patterns

To quantify the temporal diversity of responses in the SNpr, we calculated the correlations between activity on different trials (Figure 2 and see STAR Methods for more details). Figure 2A depicts a neuron presenting a diverse temporal pattern. We first smoothed the activity in each trial with a Gaussian filter (SD 30 ms, see Figure S1 for other SDs) and then calculated the correlation matrix between all trials (Figure 2B). Trials were ordered by direction of movement. Hence the pattern of squares along the diagonal in the correlation matrix indicates that trials from the same condition tended to have a correlated response pattern. The squares off-diagonal show the correlations under different conditions. For each of the two conditions, we defined the *between* score as the average of all the single-trial correlations between conditions. This is depicted in Figure 2C in the black square representing the mask of all the values averaged for conditions *i* and *j*. We compared the *between* score to the *within* score, which was defined as the geometric mean of the average correlation within each condition (excluding the correlation of a trial with itself). This is represented in Figure 2C by the triangles near the diagonal that mask the values averaged to calculate the *within* score. In the Appendix, we show that the ratio of the *between* to the *within* scores equals the correlation between the average temporal pattern of the responses. Therefore, a ratio of 1 indicates linear scaling of the responses across conditions whereas larger *within* than *between* scores characterize diverse temporal patterns across conditions.

Figure 2D shows the *within* versus *between* scores calculated for all pairs of conditions for each neuron in the SNpr. Responses consistent across conditions (exhibiting linear scaling) resulted in large *within* and *between* scores. These fell near the equality line, far from the origin (Figure 2D dark dots showing neuron 1 from Figure 1C). Responses with diverse temporal patterns across conditions resulted in large *within* and small *between* scores. These appear beneath the equality line, far from the origin (Figure 2D in blue showing neuron 2 from Figure 1C). Finally, neurons with small responses had small *within* and *between* scores. These fell near the origin (Figure 2D in green showing neuron 3 from Figure 1C). Thus, the comparison of the *within* and *between* scores serves to differentiate the three patterns shown in Figure 1. Neurons with responses that scaled linearly plot along the diagonal, neurons with diverse temporal patterns plot beneath the diagonal, and neurons with small responses plot near the origin. Note that the latter two cannot be distinguished from the calculation of the correlations of the average activity.

Overall, we found numerous responses from the SNpr that fell far from the origin beneath the equality line (Figure 2D), indicating that neurons in the SNpr encoded different directions of movement with diverse temporal patterns. We compared the pattern of scores to the pattern expected from different values of the correlation of average activity (lines in Figure 2D). We found that many pairs of conditions matched the low average correlations. This demonstrates that many SNpr neurons coded movement direction with a rich temporal pattern of activity and hence diverged from the simple characteristic increase/decrease in activity that is classically assumed to gate or enable movement.

SNpr responses are more diverse than other cortical and subcortical populations

To test whether the diverse responses in the SNpr are specific or whether other cortical and subcortical populations also have similarly diverse responses, we calculated the *within* and *between* scores of neurons in other oculomotor areas recorded in the same monkeys; namely, the input structure of the basal ganglia (striatum) and the vermis of the cerebellum.[18] We also compared these results to neurons from the floccular complex of the cerebellum,[19] MT,[20] and frontal eye field[21] (FEF) recorded in similar tasks in other monkeys.

We binned the *within* score (i.e., Figure 2D) into quantiles and then computed the mean *within* minus *between* differences for each quantile. We denote this difference between scores (*within-between*) as the *Diversity score* since larger values indicate more diverse responses across conditions. Figure 3A shows the relationship between the *diversity* score and the *within* score during pursuit (see Figure S2A for the saccade task). This presentation highlights the regime of strong responses (*within* $\gg$ 0) in which there was a clear difference in the

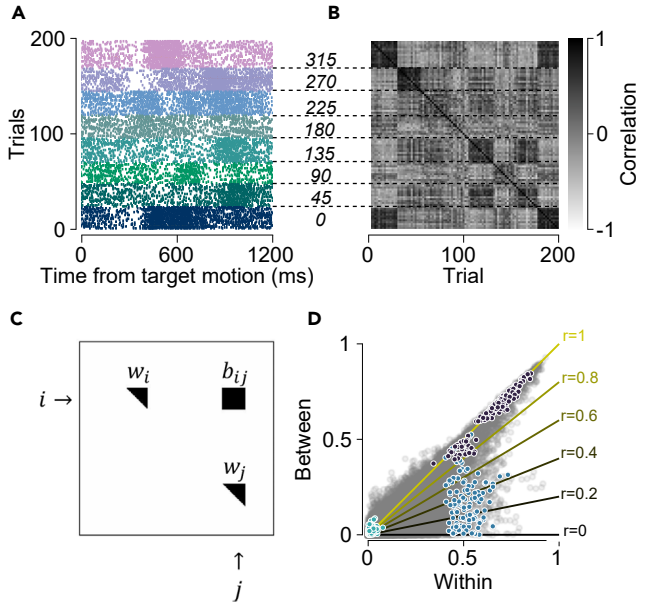

Figure 2. Diversity of SNpr responses as indicated by the Within vs. Between scores

(A) Raster of a single neuron. Each row is the activity of a single trial during the target motion. Dashed lines from A to B mark the condition borders with the direction of target movement in degrees. Colors represent the different directions of movement.

(B) Correlation matrix calculated over the rows of the raster matrix in A after the raster was smoothed with a Gaussian filter. The brightness of each pixel indicates the size of the correlation.

(C) Mask over the correlation matrix in B. *i* and *j* are two different conditions. The black square (labeled b_{ij}) marks the position in the correlation matrix shown in B that corresponds to the correlation of trials *between* the *i*th and *j*th condition. The triangles mark the position in the correlation matrix of the correlation *within* the *i*th and *j*th condition (labeled as w_i and w_j).

(D) Scatter of within (horizontal axis) versus between scores (vertical axis) for all neurons from the SNpr. Each dot represents a pair of conditions from individual neurons from the SNpr. Colored dots are example neurons from Figure 1C. Dark blue, blue, and green correspond to the neurons on the left, middle, and right of Figure 1C. Solid lines indicate different theoretical correlation slopes specified by the R value (see Appendix).

diversity scores. The diversity of activity patterns observed in the SNpr during pursuit was found to be significantly higher than that observed in other regions within the eye movement pathway, including the subcortical (Figure 3A) and cortical regions (Figure 3B, SNpr vs. FEF p = 5.6e-38, SNpr vs. MT 1.1e-11, SNpr vs. Striatum p = 1.3e-10, SNpr vs. Vermis p = 5.7e-88, SNpr vs. Flocculus p = 8.8e-52 Wilcoxon signed-rank test, see STAR Methods). We also found that for very large *within* scores, the temporal diversity of SNpr decreased. This indicates that in addition to the complex responses in the SNpr there is a subpopulation with very large and stereotypic responses (e.g., Figure 2D, dark dots).

The diversity of responses depends on sensorimotor parameters

The SNpr responses were more diverse during pursuit than during saccades (Figure 3C, p = 9.1e-59, Wilcoxon signed-rank test see STAR Methods), indicating that diversity depends on the sensorimotor profile of the behavior. To further characterize the relationship between diversity and the sensorimotor properties of the movement we compared similarity in temporal pattern as a function of similarity in movement direction. The diversity of the response increased with the difference in the angle of movement (Figure 3D, see Figure S2B for saccade).

We performed controls to verify that the diversity did not result from the pattern of catch-up saccades during pursuit. Figure S3A (top) shows examples of the pattern of catch-up saccades during pursuit. Evidently, saccades are sparse within pursuit. This prompted a first control in which we treated the time around the catch-up saccade as missing data and found that this had very little impact on diversity (Figure S3B). In addition, the timing of the saccade was predominantly distributed randomly across the trial, both within and between conditions (Figure S3A bottom). Any response that is inconsistent temporally across trials would contribute to the trial-by-trial variability rather than the average response and thereby result in a proportional decrease in the within and between scores, which would not lead to an increase in the diversity score (see Appendix). This observation prompted a second control, in which we calculated the diversity of eye speeds across directions of movement. This diversity was low (Figure S3C), indicating that it could not account for the diversity observed in SNpr. In addition, we did not find oscillation in the eye movement that was consistent across trials[22] indicating that diversity cannot be attributed to such oscillation.

The diversity of responses to rewards varies as a function of different task epochs

We compared response activity across different reward probabilities. The color of the targets indicating the probability of reward appeared in the cue epoch (see Figure 1A) and persisted throughout the motion epoch. Figure 4A shows the response of a neuron that responded

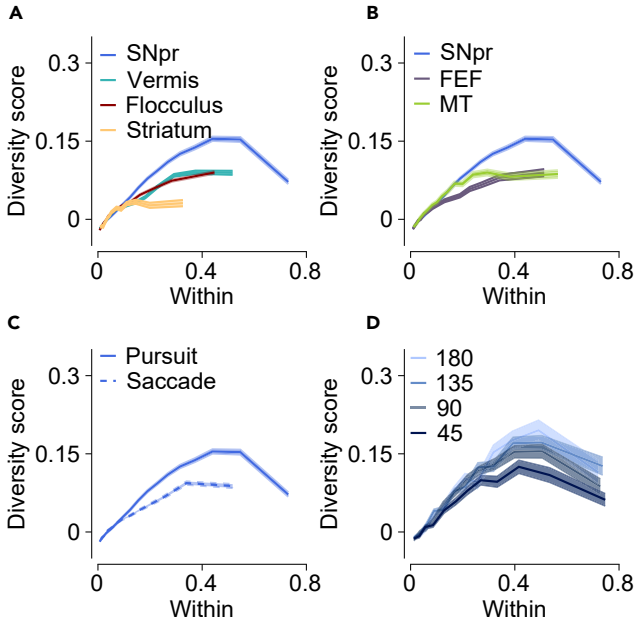

Figure 3. Temporal diversity of SNpr neurons exceeds other populations

(A–D) Each plot shows the diversity scores (within-between, vertical axis), as a function of the within score (horizontal axis). The horizontal axis was binned into quantiles (15 bins). Error bands indicate SEM. A and B. Comparison of the SNpr with subcortical (A) and cortical (B) regions. Colors indicate different neural populations. (C) Comparison between saccade (dashed line) and pursuit (solid line) tasks in the SNpr. (D) Comparison between distances in target motion direction in the SNpr. Colors indicate the angle between conditions.

differentially to the appearance of color cues. The raster of this neuron shows that the response was consistent across trials within a condition. The PSTH of the response shows that the temporal patterns of these responses were not a linear combination of each other (CC = 0.11). We calculated the *within* and *between* scores for this neuron and found that indeed the *within* score was substantially larger than the *between* score (Figure 4B, yellow dots). Note that at the time of the cue the monkey did not know the direction of the upcoming motion. Nevertheless, we calculated the scores separately for the different upcoming movement directions to enhance comparison with the diversity of the reward probability during movement (8 yellow dots corresponding to 8 directions of upcoming motion rather than 1 in Figure 4B).

Figure 4B illustrates the *within* versus *between* scores for all SNpr neurons during the motion epoch and the cue epoch (depicted in dark and light blue). Many scores calculated during the cue fell below the equality line, whereas during motion, the scores were mostly distributed along the equality line, indicating greater diversity between reward probability conditions during the cue epoch. As previously, we calculated the diversity score and plotted it as a function of the *within* score (Figure 4C). As expected from the small reward-probability modulations during movement[18] we did not find diverse reward-related responses, as indicated by the low diversity scores across reward probability conditions (Figure 4C, dark blue). This also confirms the validity of grouping responses with different reward probabilities in the movement epoch. By contrast, in the cue epoch when the color target appeared and the monkeys were fixating on the target, we found diverse responses (Figure 4C), thus indicating that diversity in patterns of activity is not limited to the coding of movement direction. We also calculated the diversity score of the responses to reward probability in the other subcortical populations (Figure S4). All populations showed increases diversity during cue in comparison to the movement. We did not find major differences between the populations, yet the substantially larger responses of the SNpr to the color cue[18] limited the regime of the *within* score of these comparisons.

Multidimensional responses of single neurons in the SNpr

The low correlation in the pairs of neural responses suggests that the neural responses across movement directions cannot be described by a single temporal pattern. Thus, the neural code for movement direction is likely to contain a large number of distinct temporal patterns of activity. These temporal patterns can be conceptualized as dimensions within the activity space of a single neuron, where higher dimensionality signifies an increased capacity for representing a greater range of functions within the activity space. To quantify this dimensionality, we developed an analysis to estimate the number of independent dimensions required to explain the temporal pattern of the neuronal response (Figure 5A, see STAR methods). This analysis first involved computing the PSTH of each condition. We then calculated the total variance in the PSTH matrix ($\tilde{\sigma}$) to serve as a statistic for computing the dimensionality. To assess the significance of $\tilde{\sigma}$, we generated a distribution of variances by shuffling the trial conditions before computing the PSTHs. If $\tilde{\sigma}$ was significant, we moved to the next dimension by eliminating the activity from the neural responses in the direction exhibiting the highest variance (1st principal component) within the PSTH matrix. This

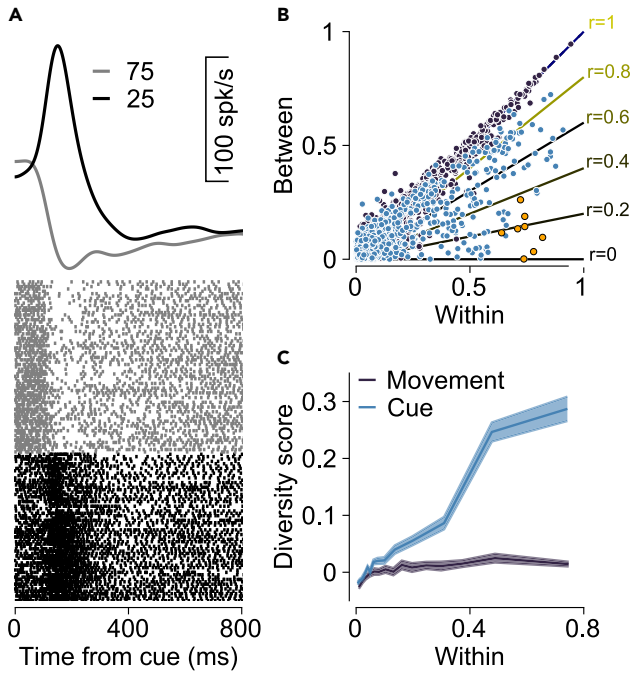

Figure 4. The diversity of responses to reward probability is larger for the cue than movement

(A) PSTH (top), and raster (bottom) of the response of an example neuron from the SNpr to the color cue appearance. Colors indicate reward probability.

(B) Scatter of within (horizontal axis) versus between scores (vertical axis) for all neurons from the SNpr. Each dot represents the pair of probability conditions during cue (light blue) and target-motion (dark blue) epochs. Orange dots correspond to the neuron in A. Solid lines indicate different theoretical correlation slopes specified by the R value (see Appendix).

(C) Comparison of reward probability diversity during cue (light blue) and movement (dark blue). Error bands indicate SEM.

process continued until the variance across PSTHs was no longer significant, yielding an estimate of the number of dimensions required to explain the variability of the neuronal response.

We validated through simulations that across a broad spectrum of noise conditions the algorithm identified the correct number of dimensions (Figures 5B and 5C, see STAR Methods for simulation details). In this analysis, responses characterized by linear scaling, akin to the characteristic examples of tuning curves[23] are attributed a dimension of 1. Figure 1C (left) presents a neuron demonstrating a singular dimension, characterized by the evident linear scaling observed in the later phase of its response. Responses displaying more intricate patterns correspond to dimensions larger than 1. For instance, the neuron in Figure 1C (middle) exhibited a dimension of 5. Finally, neurons that respond identically across all condition are assigned a dimension of 0. To differentiate neurons that exhibited non-responsiveness (e.g., Figure 1C, right plot) from neurons that exhibited stereotypical responses in all directions, we conducted an F-test on spike counts within time bins (see STAR Methods). Neuron that did not pass the significance criteria ($p = 0.05$) were classified as non-responsive (NR).

We found that 56% of the SNpr neurons had a dimension of 2 or more during pursuit (Figures 6A and 6B, see Figure S5 for saccade). The SNpr trace plotted the lowest in the cumulative distribution of dimensions, indicating that the activity of SNpr neurons had higher dimensions than the other populations (Figures 6A and 6B, SNpr vs. vermis $p = 6.8e\text{-}16$, SNpr vs. flocculus $p = 2.2e\text{-}30$, SNpr vs. Striatum $p = 2.0e\text{-}29$, SNpr vs. FEF $p = 9.9e\text{-}21$, SNpr vs. MT $p = 1.7e\text{-}5$ Wilcoxon rank-sum), enabling them to span a broader range of functions. Moreover, the dimension analysis for the SNpr neurons revealed a higher dimension during the pursuit than during saccades (Figure 6C, SNpr pursuit vs. SNpr saccade $p = 7.2e\text{-}10$, Wilcoxon rank-sum), indicating that individual SNpr neuron diversity depends on the sensorimotor profile of behavior.

To confirm that the higher dimensions observed in the SNpr were not simply a result of larger responses, we calculated the effect size (see STAR Methods)[18] of each neuron and compared the dimensions of the SNpr to those of other brain areas involved in eye movements. We found that even when controlling for effect size, SNpr neurons had significantly higher dimensions than the other populations (Figures 6D and 6E, SNpr vs. striatum $p = 1.1e\text{-}5$, SNpr vs. FEF $p = 2.1e\text{-}8$, SNpr vs. vermis $p = 0.01$, SNpr vs. flocculus $p = 7.1e\text{-}8$, SNpr vs. MT $p = 2.9e\text{-}11$ Wilcoxon signed-rank test, see STAR Methods). Comparing the dimensions of the SNpr neurons for similar effect sizes during the pursuit and saccade tasks yielded a higher dimensionality in the responses when the monkeys performed pursuit eye movement task (Figure 6F, $p = 3.3e\text{-}4$ Wilcoxon signed-rank test, see STAR Methods). Thus, SNpr temporal diversity was related to the behavior, with higher diversity during pursuit. During saccades the difference between populations was less pronounced (Figure S5), indicating that the examination of pursuit behavior was key to revealing the access diversity of the SNpr.

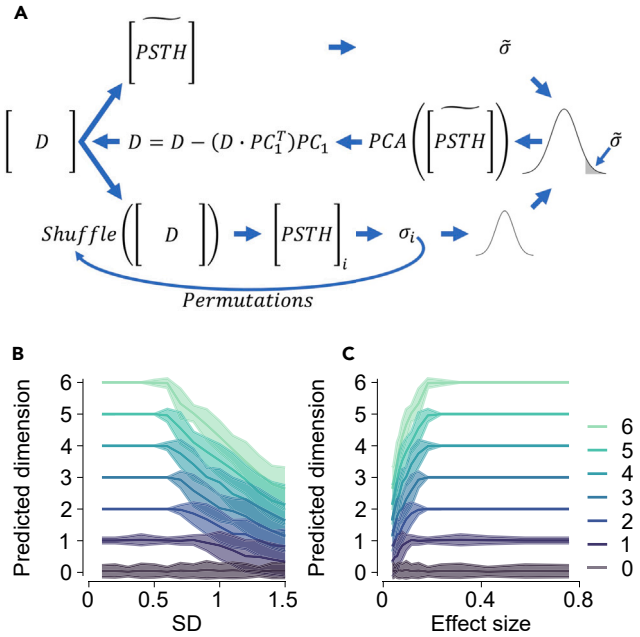

Figure 5. Dimension analysis and simulation

(A) Schematic dimension analysis where arrows indicate the sequential steps in the analysis. The D matrix represents the data matrix of all trials across time. The upper part shows the computation of the PSTH and statistics marked with a tilde. The lower part represents the computation of a distribution for the statistical tests. The *i*th PSTH and sigma are generated by shuffling the D conditions, to generate a distribution of sigma. The sigma tilde is compared to the distribution (middle row on the right), and if significant, the first PC (PC1) of PSTH tilde is extracted and all the variance of D in the direction of PC1 is subtracted (middle). The analysis is repeated with the updated D matrix.

(B) Results of a simulation validating the dimension analysis. The predicted dimension (vertical axis) as a function of the standard deviation of the noise (horizontal axis). The color indicates the true dimension, lines show averages, and bands indicate the standard deviation across 100 simulations.

(C) The predicted dimension (vertical axis) as a function of the effect size of the simulated neurons (horizontal axis). Colors and bands are the same as in B.

DISCUSSION

We found that the SNpr neurons exhibited highly diverse reaction patterns during movement, including frequent increases and decreases in firing rate, as well as uncorrelated responses in different directions and reward conditions resulting in the high dimensional activity of single neurons. The activity in SNpr was more diverse than in other cortical and subcortical areas in the pursuit eye movement system. Furthermore, the pattern of SNpr activity differed from the patterns of eye motoneuronal activity which were linearly related to the projection of the eye velocity and position in the preferred direction of muscle activity (Figure S6).[24–26] Thus, the activity in the SNpr did not match the pattern needed to excite or inhibit single motoneuronal activity.

While many neurons in the SNpr demonstrated high-dimensional encoding, our findings also included subpopulation responses with typical pauses during motion (see Figure 3A). These responses aligned better with the description of neurons performing a gating role. The presence of these two response patterns within different subpopulations might be attributed to the two efferent connections of the SNpr. The SNpr has an efferent connection to the thalamus[27,28] and the superior colliculus.[29] This raises the possibility that the SNpr may serve both as a gatekeeper for the superior colliculus by transmitting gating responses, and as a pathway for sending temporally diverse high-dimensional sensorimotor information to the thalamus and thereby to the cerebral cortex. Our results suggest a dynamic complex mapping between sensorimotor parameters and activity, hinting at the involvement of the SNpr in more sophisticated neural computations, possibly through its connections to the thalamus. Diverse and high-dimensional neural responses offer benefits by enabling extensive classification through simple linear readouts,[30–32] and can encompass a wide range of behavioral functions. Our results suggest that the SNpr is capable of engaging in the separation and classification of task-related information and embedding it in a high-dimensional space that creates opportunities for versatile and diverse high-level task performance.

The mechanism underlying the emergence of diversity in the basal ganglia remains a topic of investigation. Studies of the arm movement system have posited that diversity arises from an autonomous dynamical system implemented through local recurrent connectivity[33,34] (but see in the study by Sauerbrei et al.[35]). However, unlike the arm movement system, the initiation and maintenance of the pursuit system rely heavily on visual inputs, suggesting that the observed diversity during pursuit is more likely to arise from the way visual inputs are processed and integrated by the neural circuitry rather than being solely dependent on local recurrent connectivity. Although the basal ganglia exhibit local reverberating connectivity that could generate temporal diversity, the output nuclei are mostly driven by feedforward inputs via direct and indirect pathways from the striatum and the hyper-direct pathways from the cortex.[1] Thus, our results suggest that diversity in output is achieved

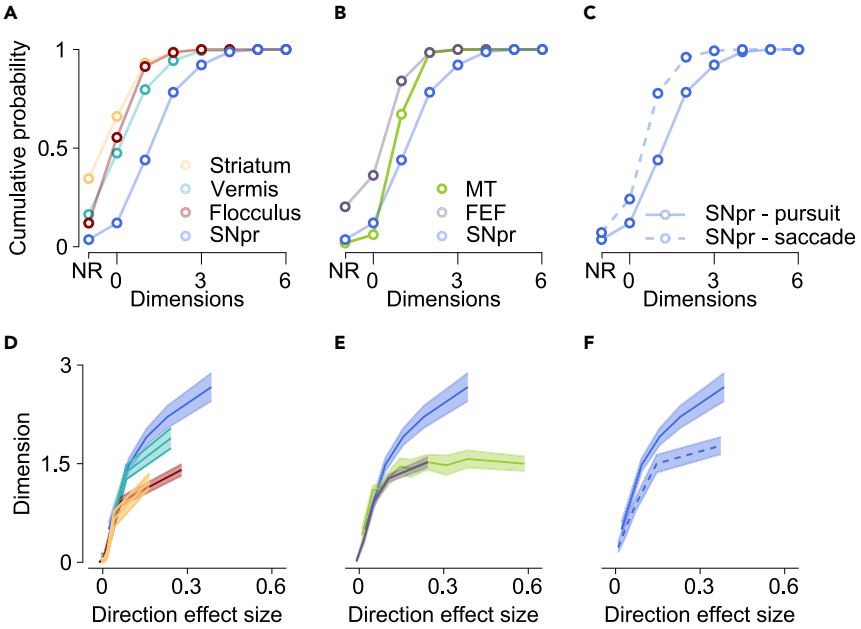

Figure 6. Dimensionality of neurons in the SNpr exceeds other populations

(A–C) Cumulative distribution of neuron dimensionality. (A and B) Comparisons of SNpr neurons versus subcortical (A) and cortical regions (B). Non-responsive (NR) neurons constitute a subset within the dimension 0 category that did not significantly respond during target motion (see STAR Methods). Colors represent different populations. (C) Comparison of SNpr during pursuit (solid line) versus saccade (dashed line).

(D–F) Dimensionality as a function of effect size. (D and E) Comparisons of SNpr neurons versus subcortical (D) and cortical regions (E). Error bands indicate SEM. Colors are the same as in (A and B). (F) Comparison of SNpr during pursuit (solid line) versus saccade (dashed line). Error bands indicate SEM.

through connectivity between areas rather than local recurrent connectivity. The lower diversity of the striatal neuron (Figures 3A and 6D) suggests that diversity arises from the pattern of convergence. A regression analysis (not shown) further confirmed that diversity responses in the SNpr can be predicted from the many striatal neurons supporting the role of inputs rather than *de novo* generation of diversity in the SNpr.

Limitation of the study

The results of the current study hold promise for further exploration in several critical directions. We studied diversity in the coding of movement direction during saccades and pursuit. Despite our efforts to address potential explanations for the diverse responses observed during the pursuit, such as catch-up saccades or systematic ringing eye movements, complete characterization of sensorimotor factors that contribute to the diversity remains challenging. Future research could examine the ways in which diversity is related to other parameters of movement, such as duration or speed, and probe more densely the direction of movement. We found diverse responses even in the closest direction of movement (Figure 3D), suggesting discontinuity in the coding of movement direction. Identifying and characterizing these discontinuities could provide further insights into the coding of movement direction. In addition, we compared diversity in the SNpr to inputs from the striatum and other brain regions outside the basal ganglia. A compelling avenue for future research would be to compare this diversity to outputs of the SNpr, specifically by comparing with the superior colliculus and thalamus to study how the diverse activity is readout by downstream structures. Finally, further characterization of the inputs to the SNpr such as dissection of the inputs from the external segment of the globus pallidus or subthalamic nucleus or selective probing of direct and indirect pathways[7,36] could characterize how diversity arises within the basal ganglia.

STAR★METHODS

Detailed methods are provided in the online version of this paper and include the following:

- KEY RESOURCES TABLE
- RESOURCE AVAILABILITY
  - Lead contact
  - Materials availability
  - Data and code availability
- EXPERIMENTAL MODEL AND STUDY PARTICIPANT DETAILS
- METHOD DETAILS
  - Experimental design

- QUANTIFICATION AND STATISTICAL ANALYSIS
  - Saccade detection
  - PSTH calculation
  - Analysis of between and within scores
  - Testing neuronal measures using score matching
  - Dimension analysis
  - Effect size
  - Appendix

SUPPLEMENTAL INFORMATION

Supplemental information can be found online at https://doi.org/10.1016/j.isci.2024.110667.

ACKNOWLEDGMENTS

This work is dedicated to the memory of Mrs. Lily Safra, a great supporter of brain research. We thank Stephen. G Lisberger, in whose laboratory the MT data were collected. This project received funding from the European Research Council (ERC) under the European Union's Horizon 2020 research and innovation program (grant agreement No 755745) and the Israel Science Foundation (380/17).

AUTHOR CONTRIBUTIONS

G.Z., N.L., and M.J. designed the experiment, conducted data analysis, and co-authored the manuscript. G.Z. and N.L. performed data collection for the striatum, SNpr, and vermis. M.C. collected data from the FEF, and M.J. contributed motoneuron data. A.L. and M.Y. provided data from the flocculus, and S.B. contributed MT data.

DECLARATION OF INTERESTS

The authors declare no competing interests.

DECLARATION OF GENERATIVE AI AND AI-ASSISTED TECHNOLOGIES IN THE WRITING PROCESS

During the preparation of this work, the authors used ChatGPT for English editing and Bing for creating non-scientific illustrations in the graphical abstract. After using these tools/services, the authors reviewed and edited the content as needed and take full responsibility for the content of the publication.

Received: October 26, 2023
Revised: April 8, 2024
Accepted: August 1, 2024
Published: August 3, 2024

REFERENCES

1. Redgrave, P., Rodriguez, M., Smith, Y., Rodriguez-Oroz, M.C., Lehericy, S., Bergman, H., Agid, Y., Delong, M.R., and Obeso, J.A. (2010). Goal-directed and habitual control in the basal ganglia: implications for Parkinson's disease. Nat. Rev. Neurosci. *11*, 760–772. https://doi.org/10.1038/nrn2915.
2. DeLong, M.R. (1990). Primate models of movement disorders of basal ganglia origin. Trends Neurosci. *13*, 281–285. https://doi.org/10.1016/0166-2236(90)90110-V.
3. Hikosaka, O., Takikawa, Y., and Kawagoe, R. (2000). Role of the basal ganglia in the control of purposive saccadic eye movements. Physiol. Rev. *80*, 953–978. https://doi.org/10.1152/PHYSREV.2000.80.3.953/ASSET/IMAGES/LARGE/9J0300083007.JPEG.
4. Joshua, M., Adler, A., Rosin, B., Vaadia, E., and Bergman, H. (2009). Encoding of probabilistic rewarding and aversive events by pallidal and nigral neurons. J. Neurophysiol. *101*, 758–772. https://doi.org/10.1152/JN.90764.2008/ASSET/IMAGES/LARGE/Z9K0020992970010.JPEG.
5. Shin, S., and Sommer, M.A. (2010). Activity of neurons in monkey globus pallidus during oculomotor behavior compared with that in substantia nigra pars reticulata. J. Neurophysiol. *103*, 1874–1887. https://doi.org/10.1152/JN.00101.2009/ASSET/IMAGES/LARGE/Z9K0041000190012.JPEG.
6. Mink, J.W. (1996). The basal ganglia: focused selection and inhibition of competing motor programs. Prog. Neurobiol. *50*, 381–425. https://doi.org/10.1016/S0301-0082(96)00042-1.
7. Cui, G., Jun, S.B., Jin, X., Pham, M.D., Vogel, S.S., Lovinger, D.M., and Costa, R.M. (2013). Concurrent activation of striatal direct and indirect pathways during action initiation. Nature *494*, 238–242. https://doi.org/10.1038/nature11846.
8. Churchland, M.M., Cunningham, J.P., Kaufman, M.T., Foster, J.D., Nuyujukian, P., Ryu, S.I., Shenoy, K.V., and Shenoy, K.V. (2012). Neural population dynamics during reaching. Nature *487*, 51–56. https://doi.org/10.1038/nature11129.
9. Mante, V., Sussillo, D., Shenoy, K.V., and Newsome, W.T. (2013). Context-dependent computation by recurrent dynamics in prefrontal cortex. Nature. Com *503*, 78–84.
10. Joshua, M., Medina, J.F., and Lisberger, S.G. (2013). Diversity of Neural Responses in the Brainstem during Smooth Pursuit Eye Movements Constrains the Circuit Mechanisms of Neural Integration. J. Neurosci. *33*, 6633–6647. https://doi.org/10.1523/JNEUROSCI.3732-12.2013.
11. Robinson, D.A. (1981). The use of control systems analysis in the neurophysiology of eye movements. Annu. Rev. Neurosci. *4*, 463–503.
12. Sparks, D.L. (2002). The brainstem control of saccadic eye movements. Nat. Rev. Neurosci. *3*, 952–964. https://doi.org/10.1038/nrn986.
13. Handel, A., and Glimcher, P.W. (1999). Quantitative analysis of substantia nigra pars reticulata activity during a visually guided saccade task. J. Neurophysiol. *82*, 3458–3475. https://doi.org/10.1152/JN.1999.82.6.3458/ASSET/IMAGES/LARGE/9K1190557019.JPEG.
14. Hikosaka, O., and Wurtz, R.H. (1983). Visual and oculomotor functions of monkey substantia nigra pars reticulata. I. Relation of visual and auditory responses to saccades.

J. Neurophysiol. *49*, 1230–1253. https://doi.org/10.1152/JN.1983.49.5.1230.
15. Basso, M.A., Pokorny, J.J., and Liu, P. (2005). Activity of substantia nigra pars reticulata neurons during smooth pursuit eye movements in monkeys. Eur. J. Neurosci. *22*, 448–464. https://doi.org/10.1111/J.1460-9568.2005.04215.X.
16. Basso, M.A., and Sommer, M.A. (2011). Exploring the role of the substantia nigra pars reticulata in eye movements. Neuroscience *198*, 205–212. https://doi.org/10.1016/J.NEUROSCIENCE.2011.08.026.
17. Rashbass, C. (1961). The relationship between saccadic and smooth tracking eye movements. J. Physiol. *159*, 326–338. https://doi.org/10.1113/JPHYSIOL.1961.SP006811.
18. Larry, N., Zur, G., and Joshua, M. (2024). Organization of reward and movement signals in the basal ganglia and cerebellum. Nat. Commun. *15*, 2119. https://doi.org/10.1038/s41467-024-45921-9.
19. Lixenberg, A., Yarkoni, M., Botschko, Y., and Joshua, M. (2020). Encoding of eye movements explains reward-related activity in cerebellar simple spikes. J. Neurophysiol. *123*, 786–799. https://doi.org/10.1152/JN.00363.2019/ASSET/IMAGES/LARGE/Z9K0032053720008.JPEG.
20. Behling, S., and Lisberger, S.G. (2023). A sensory-motor decoder that transforms neural responses in extrastriate area MT into smooth pursuit eye movements. J. Neurophysiol. *130*, 652–670. https://doi.org/10.1152/JN.00200.2023/ASSET/IMAGES/LARGE/JN.00200.2023_F013.JPEG.
21. Cain, M., and Joshua, M. (2023). Population coding of distinct categories of behavior in the frontal eye field. Preprint at bioRxiv. https://doi.org/10.1101/2023.11.28.568997.
22. Goldreich, D., Krauzlis, R.J., and Lisberger, S.G. (1992). Effect of changing feedback delay on spontaneous oscillations in smooth pursuit eye movements of monkeys. J. Neurophysiol. *67*, 625–638. https://doi.org/10.1152/JN.1992.67.3.625.
23. Georgopoulos, A.P., Schwartz, A.B., and Kettner, R.E. (1986). Neuronal Population Coding of Movement Direction. Science *233*, 1416–1419. https://doi.org/10.1126/SCIENCE.3749885.
24. Sylvestre, P.A., and Cullen, K.E. (1999). Quantitative analysis of abducens neuron discharge dynamics during saccadic and slow eye movements. J. Neurophysiol. *82*, 2612–2632. https://doi.org/10.1152/JN.1999.82.5.2612/ASSET/IMAGES/LARGE/9K1190582016.JPEG.
25. Ghasia, F.F., and Angelaki, D.E. (2005). Do Motoneurons Encode the Noncommutativity of Ocular Rotations? Neuron *47*, 281–293. https://doi.org/10.1016/J.NEURON.2005.05.031.
26. Fuchs, A.F., and Luschei, E.S. (1970). Firing patterns of abducens neurons of alert monkeys in relationship to horizontal eye movement. J. Neurophysiol. *33*, 382–392. https://doi.org/10.1152/JN.1970.33.3.382.
27. Partanen, J., and Achim, K. (2022). Neurons gating behavior—developmental, molecular and functional features of neurons in the Substantia Nigra pars reticulata. Front. Neurosci. *16*, 976209. https://doi.org/10.3389/FNINS.2022.976209/FULL.
28. Calabresi, P., Picconi, B., Tozzi, A., Ghiglieri, V., and Di Filippo, M. (2014). Direct and indirect pathways of basal ganglia: a critical reappraisal. Nature *17*, 1022–1030.
29. Krauzlis, R.J. (2004). Recasting the Smooth Pursuit Eye Movement System. J. Neurophysiol. *91*, 591–603. https://doi.org/10.1152/JN.00801.2003.
30. Rigotti, M., Rubin, D.B.D., Wang, X.J., and Fusi, S. (2010). Internal representation of task rules by recurrent dynamics: The importance of the diversity of neural responses. Front. Comput. Neurosci. *4*, 24. https://doi.org/10.3389/FNCOM.2010.00024.
31. Fusi, S., Miller, E.K., and Rigotti, M. (2016). Why neurons mix: high dimensionality for higher cognition. Curr. Opin. Neurol. *37*, 66–74.
32. Rigotti, M., Barak, O., Warden, M.R., Wang, X.J., Daw, N.D., Miller, E.K., and Fusi, S. (2013). The importance of mixed selectivity in complex cognitive tasks. Nature *497*, 585–590.
33. Sussillo, D., Churchland, M.M., Kaufman, M.T., and Shenoy, K.V. (2015). A neural network that finds a naturalistic solution for the production of muscle activity. Nat. Neurosci. *18*, 1025–1033. https://doi.org/10.1038/nn.4042.
34. Churchland, M.M., Cunningham, J.P., Kaufman, M.T., Ryu, S.I., and Shenoy, K.V. (2010). Cortical Preparatory Activity: Representation of Movement or First Cog in a Dynamical Machine? Neuron *68*, 387–400. https://doi.org/10.1016/j.neuron.2010.09.015.
35. Sauerbrei, B.A., Guo, J.Z., Cohen, J.D., Mischiati, M., Guo, W., Kabra, M., Verma, N., Mensh, B., Branson, K., and Hantman, A.W. (2020). Cortical pattern generation during dexterous movement is input-driven. Nature *577*, 386–391. https://doi.org/10.1038/s41586-019-1869-9.
36. Kravitz, A.V., Freeze, B.S., Parker, P.R.L., Kay, K., Thwin, M.T., Deisseroth, K., and Kreitzer, A.C. (2010). Regulation of parkinsonian motor behaviours by optogenetic control of basal ganglia circuitry. Nature *466*, 622–626. https://doi.org/10.1038/nature09159.
37. Schultz, W. (1986). Activity of pars reticulata neurons of monkey substantia nigra in relation to motor, sensory, and complex events. J. Neurophysiol. *55*, 660–677. https://doi.org/10.1152/JN.1986.55.4.660.
38. Larry, N., Yarkoni, M., Lixenberg, A., and Joshua, M. (2019). Cerebellar climbing fibers encode expected reward size. Elife *8*, e46870. https://doi.org/10.7554/ELIFE.46870.
39. Lixenberg, A., and Joshua, M. (2018). Encoding of Reward and Decoding Movement from the Frontal Eye Field during Smooth Pursuit Eye Movements. J. Neurosci. *38*, 10515–10524. https://doi.org/10.1523/JNEUROSCI.1654-18.2018.
40. Rashbass, C., and Westheimer, G. (1961). Independence of conjugate and disjunctive eye movements. J. Physiol. *159*, 361–364.
41. Behling, S., and Lisberger, S.G. (2020). Different mechanisms for modulation of the initiation and steady-state of smooth pursuit eye movements. J. Neurophysiol. *123*, 1265–1276. https://doi.org/10.1152/JN.00710.2019.
42. Olejnik, S., and Algina, J. (2003). Generalized Eta and Omega Squared Statistics: Measures of Effect Size for Some Common Research Designs. Psychol. Methods *8*, 434–447. https://psycnet.apa.org/fulltext/2003-10163-005.pdf.
43. Okada, K. (2013). Is omega squared less biased? A comparison of three major effect size indices in one-way ANOVA. Springer *40*, 129–147.
44. Olejnik, S., and Algina, J. (2000). Measures of effect size for comparative studies: Applications, interpretations, and limitations. Contemp. Educ. Psychol. *25*, 241–286. https://doi.org/10.1006/ceps.2000.1040.

STAR★METHODS

KEY RESOURCES TABLE

REAGENT or RESOURCE	SOURCE	IDENTIFIER
Software and algorithms		
OmniPlex	Plexon	https://plexon.com/plexon-systems/omniplex-neural-recording-system/
Plexon spike sorter	Plexon	https://plexon.com/products/offline-sorter/
Python 3.10	Python Software Foundation	https://www.python.org/downloads/release/python-3100/
MATLAB R2021b	MATLAB	https://www.mathworks.com/products/new_products/release2021b.html

RESOURCE AVAILABILITY

Lead contact

Further information and requests for resources should be directed to and will be fulfilled by the lead contact, Gil Zur (gil.zur1@mail.huji.ac.il).

Materials availability

All recordings presented in this paper are available upon request from the lead contact.

Data and code availability

- All data reported in this paper will be shared by the lead contact upon request.
- This paper does not report original code.
- Any additional information required to reanalyze the data reported in this paper is available from the lead contact upon request.

EXPERIMENTAL MODEL AND STUDY PARTICIPANT DETAILS

Data for the SNpr, striatum, vermis, flocculus, and FEF were collected in the Hebrew University of Jerusalem from two male and three female Macaca fascicularis monkeys, aged 4 to 10 years and weighing 3 to 7 kg. The experimental procedures were approved by the Institutional Animal Care and Use Committees of the Hebrew University of Jerusalem (approval numbers- MD1514585, MD1815569).

The data collected from area MT were collected in Duke university[20] from two male rhesus macaque monkeys, aged 8 to 16 years and weighing 9 to 12 kg. The experimental procedures were approved by the Institutional Animal Care and Use Committee (IACUC) of Duke university (approval number- A016-24-01).

METHOD DETAILS

The main dataset was collected from the SNpr, cerebellum and striatum of a female (Monkey G) and a male (Monkey A) Macaca fascicularis monkey that had been prepared for behavior, and equipped for neural recording using techniques described in detail previously.[18] Briefly, we implanted head holders to restrain the monkeys' heads and trained the monkeys to track spots of light that moved across a video monitor positioned in front of them (55 cm and 63 cm from the eyes of monkeys A and G). We used liquid food rewards (baby food mixed with water and infant formula), delivered from a tube placed in front of the monkeys, to reward them for accurate tracking of the targets. The position of the eye was continuously tracked during the recording.

We performed two subsequent surgeries to place a 19 mm diameter cylindrical recording over the basal ganglia and the vermis. We first recorded from the caudate and then moved on to the SNpr, while continuously recording from the vermis. Based on an extensive mapping of the caudate and an MRI image of the brain, we estimated the location of the SNpr in the recording chamber. Then, we lowered the electrodes to this location. At the targeted site, we identified neurons with a high baseline firing rate and the typical extracellular shape of SNpr neurons.[37] We confirmed that some of these neurons exhibited a clear pause during saccades in certain directions. On some recording days, we also identified neurons with pronounced eye position sensitivity in nearby areas, as expected from the neighboring third oculomotor nerve. We used two Mini- Matrix Systems (Thomas Recording GmbH) to lower quartz-insulated tungsten electrodes (impedance of 1–2 Mohm) into the basal ganglia and cerebellum. The neural signals were digitized at a sampling rate of 40 kHz using the OmniPlex system (Plexon) and sorted offline (Plexon spike sorter). We only used neurons that displayed distinct clusters of waveforms in the sorting procedure. The sorted spikes were converted into time stamps with a resolution of 1 ms and were inspected again visually to identify any instability or obvious errors in the sorting procedure. To control for potential behavioral differences between reward conditions that might affect our results, we also recorded the monkeys' licking behavior. We used an infrared beam to track the licks. Monkey A tended not to extend its tongue, so we recorded its lip movements instead.

We compared the main dataset from the SNpr, cerebellum and striatum to other datasets from the FEF, Flocculus and MT. These datasets were obtained in slightly different tasks (see below) using similar recording techniques that were reported previously.[20,21,38,39]

Experimental design

Pursuit task

Each trial started with a bright white target that appeared in the center of the screen (Figure 1A). After 500 ms of presentation, in which the monkey was required to acquire and maintain fixation, a colored target replaced the fixation target. The color of the target signaled the probability of receiving a reward upon successful tracking of the target. For monkey A we used yellow to indicate a 75% for reward and green to indicate 25%. For monkey G we reversed the associations. After a variable delay of 800–1200 ms, the targets stepped in one of eight directions (0°, 45°, 90°, 135°, 180°, 225°, 270°, 315°; the same directions were used for all tasks below) and then moved continuously in the opposite direction (step-ramp).[40] For both monkeys, we used a target motion of 20°/s and a step to a position 4° from the center of the screen. The target moved for 750 ms (650 ms for 3 Striatum neurons) then stopped and stayed still for an additional 500–700 ms. If the monkey's gaze was within a 3–5°x3-5° window around the target, the monkey received a reward according to the probability specified by the color.

We confirmed that the monkeys were able to associate the color of the target and the probability of the reward[18] in another task where they were required to choose between two targets. In more than 97% of the trials the monkeys chose the 0.75 over the 0.25 probability target.

Saccade task

The structure of the saccade task was identical to the pursuit task, except for the target motion epoch. In the saccade task, following the random delay, the central colored target disappeared and immediately reappeared in one of eight eccentric locations 10° from the center of the screen. If the monkey's gaze was within a 5 ° × 5 ° window around the target, the monkey received a reward according to the probability specified by the color.

Flocculus reward size task

We analyzed data recorded from the floccular complex and adjacent areas,[38,39] while the monkeys performed a smooth pursuit task in which we manipulated reward size.[40,41] The temporal and target motion properties of the task were the same as the reward probability pursuit task described above. However, in this task, the color of the target signaled the size of the reward the monkey would receive if it tracked the target. One color was associated with a large reward (~0.2 mL) and the other with a small reward (~0.05 mL).

FEF task

We analyzed two types of trials recorded from one monkey in the FEF. In the pursuit task, the trials began with a fixation target displayed in the center of the screen. After 500 ms, an eccentric cue appeared at one of eight locations 4° away from the fixation target. This eccentric cue indicated the opposite direction of the future movement of the target. After a random delay ranging from 800 to 1200 ms, the target began to move in the direction indicated by the eccentric cue at a speed of 20° per second for 750 ms. In the saccade task, the trials began with a fixation target displayed on the screen for a random period of time ranging from 1300 to 1700 ms. Then the target jumped to one of eight eccentric locations 10° away from the center of the screen. In both tasks, the monkey received a reward at the end of the trial if it successfully followed the target.

MT task

Each trial began with a fixation dot positioned at the center of the screen for a random duration ranging from 400 to 600 ms.[20] Subsequently, a patch of dots appeared, where the dots moved locally within the patch for 100 ms at speeds of 10°/s in one of eight equally spaced directions (0°–315°). After 100 ms, the patch moved globally across the screen at the same speed and direction as the local motion, for an additional 800–1000 ms and 900–1200 ms for monkeys Ar and Di. Note that the MT dataset was collected under different conditions than other datasets. We were able to control for some of these differences (number of trials, duration of target, Figure S7); however, differences such as target speed and form could not be directly controlled. Nevertheless, based on previous documentation of MT responses[41] they were not likely to change the results substantially. We therefore present MT data while cautioning for the need for future validation.

Table 1 details the number of neurons analyzed in each task for each monkey, together with the area of recordings.

QUANTIFICATION AND STATISTICAL ANALYSIS

Analyses were performed using Python and MATLAB. To ensure accuracy, we only considered cells that had been recorded for a minimum of 100 trials in either the saccade or pursuit task. Since there were only 80 available trials in the FEF and MT region, we conducted a control analysis comparing the FEF to the SNpr region with a similar number of trials (Figure S7). Given the dynamic nature of the analyses, we paid particular attention to timing and focused on the 1200 ms time window starting from target movement onset. We evaluated the impact of taking shorter time windows after the end of the motion epoch (such as 200, 400 ms) to ensure that our results were not sensitive to this window, especially on the saccade task where movements are shorter. The length of motion was longer for MT data than for the other datasets. We therefore ran a control in which we focused our analysis on the 750 first ms after motions onset which was common to all datasets (Figure S7).

Saccade detection

We used eye velocity and acceleration thresholds to detect saccades automatically which was then verified by visual inspection of the traces. The velocity and acceleration signals were obtained by digitally differentiating the position signal after smoothing with a Gaussian filter with a standard deviation of 5 ms. Saccades were defined as an eye acceleration exceeding 1000°/s^2, an eye velocity crossing 15°/s during fixation, or an eye velocity crossing 50°/s while the target moved on the pursuit task.

PSTH calculation

To calculate the PSTH of a neuron, we first smoothed all the trials with a Gaussian filter where the standard deviation was 30 (see Figure S1 for controls with other kernel sizes). We then grouped the trials by condition and calculated the average for each group for each time point.

Analysis of between and within scores

We compared each pair of the task conditions for each neuron. For each neuron, we began our analysis with its $n \times m$ raster matrix, where n is the number of trials, and m is the number of time points in ms. We began by smoothing the activity in each trial with a Gaussian filter and then calculated the Pearson correlation matrix between all trials (i.e., row-wise correlation).

The correlation matrix was then used to define the *Within* and *Between* scores for each pair of conditions i and j as follows:

$$Within_{ij} = \sqrt{\left| \frac{1}{|w_i|} \sum_{cc \in w_i} cc \cdot \frac{1}{|w_j|} \sum_{cc \in w_j} cc \right|}$$

$$Between_{ij} = \left| \frac{1}{|b_{ij}|} \sum_{cc \in b_{ij}} cc \right|$$

where w_i is the group of all the correlations across trials in condition i (excluding correlations of a trial with itself), and b_{ij} is the group of all correlations between trials in the i-th condition and trials in the j-th condition. We defined the *Diversity* score as the *Within* minus *Between* score (*Within* -*Between*). The correlation coefficient (cc) between trials in which a neuron did not fire at all is undefined. This is especially problematic for populations that include many neurons with very low firing rates, such as the striatum. We conducted all analyses using only task conditions in which all trials had at least one spike. Additionally, we confirmed that treating the undefined CC as missing data and conducting analysis on all conditions resulted in similar conclusions.

Testing neuronal measures using score matching

To compare the *Between* score of two populations while controlling for the *Within* score we first matched each *Within* score in one population to the closest *Within* score in the other population. We then applied a Wilcoxon signed-rank for paired samples test to compare the *Between* scores of the responses that were matched by the *Within* score. Statistical significance on this test indicates that the null hypothesis that responses in the two populations with the same *Within* score have the same *Between* score is unlikely. In this analysis, we matched the population with a larger range of *Within* scores to the population with a smaller range to ensure that for each *Within* score in one population we would be able to find a close *Within* score in the other population. After matching, there were no differences between the *Within* scores of the matched population ($p > 0.15$, Wilcoxon signed-rank test).

We used this test to compare the SNpr to the other populations in the *Within-Between* analysis (Figure 3) and to compare the SNpr during pursuit and saccade. We used a similar test to compare the dimension as a function of the effect size (Figure 6), where the effect size and dimension of each neuron replaced the *Within* and *Between* Score.

Dimension analysis

We defined the dimension (d) of the responses of a neuron as follows: let D be a data matrix of a neuron, where each row of D is the activity of the neuron from a single trial. Averaging over columns of D for rows with the same trial condition result in a new matrix $PSTH_{real}$, where each row is the average activity in time during a single condition. The $PSTH_{real}$ matrix is then binned at a 100-ms interval, and the average activity in each bin is calculated. To test for the significance of the first dimension, we first calculated the total variance across $PSTH_{real}$. Next, we built a distribution of variances (1000 iterations) over multiple shuffled PSTH matrices. A shuffled PSTH matrix was generated by shuffling the trial conditions of D before averaging the PSTH as described above. The dimension was significant (i.e., d incremented by 1) if the total variance was larger than 95% of the variances generated by the shuffled PSTH matrices ($p = 0.05$). We then performed principal component analysis (PCA) on the $PSTH_{real}$ and removed all the variances in the direction of the first PC from each trial in the original data matrix (D). This was done by subtracting the projection in the direction of the first principal component of each trial:

$$D_t = D_t - \left(D_t \cdot PC_1^T\right) PC_1$$

where t is the index of the trial. By subtracting, we eliminated all the variance in the first PC direction. This enabled us to repeat the above analysis on the resulting data matrix D, where the first eigenvector was the previous second eigenvector. We proceeded until the variance

across PSTHs stopped being significant. The number of dimensions that passed the significance test (d) was defined as the dimension of the neuron. The process is illustrated in a diagram in Figure 5.

To further validate our methods, we conducted a simulation to test the performance of the response dimension method (Figure 5). We generated neurons with the same number of conditions as in our task (conditions = 16) with 10 trials per condition. The signal of each neuron was generated with a number (0–6) of orthogonal dimensions using cosine and sine functions with different frequencies; i.e., $\cos(N \cdot t)$ and $\sin(N \cdot t)$, where t represents the time between 0 and 2π and N is an integer. We added Gaussian noise (sigma range from 0.1 to 1.5) to test for the accuracy of the analysis in the presence of noise. We calculated the effect size of the simulated neurons to ensure that the dimension analyses performed well in the regime of trial-by-trial variability in the activity of the recorded neurons. The results indicated satisfactory prediction of the dimension for effect sizes exceeding ~0.2 (see Figure 5) and a monotonic relationship between the true and calculated dimensions across all ranges of effect sizes. We also compared the results of the shuffling method to a multivariate analysis of variance (MATLAB manova1). The permutation method and the MANOVA resulted in a similar estimation of the dimension. We preferred the permutation method since it can be calculated with fewer trials and does not assume that the data are drawn from a multivariate normal distribution.

Effect size

To calculate the coding of a variable throughout the entire epoch, we calculated the partial omega square (ω_p^2)[42–44] effect size. The partial effect size measures how much of the variability of a neuron is related to the experimental variable in comparison to the variability that cannot be explained by any of the variables. Here we used ω_p^2 to control the analysis of dimensions for the difference we recently found between populations in the sizes of neuron responses. Specifically, we calculated the number of spikes in 100 ms bins, 0 to 1200 ms after an event during the trial (target motion). We fitted an ANOVA model that included the direction of target motion as a variable, with the addition of time (the specific bin the sample came from). We utilized the resulting F-tests on the time bin groups within the ANOVA to distinguish neurons classified in dimension 0 into responsive and non-responsive categories.

To calculate the effect size, we used the following formula:

$$\omega_p^2 = \frac{SS_{effect} + SS_{effect\ x\ time} - \frac{df_{effect} + df_{effect\ x\ time}}{df_{error}} \cdot SS_{error}}{SS_{effect} + SS_{effect\ x\ time} + \frac{(N - df_{effect} - df_{effect\ x\ time})}{df_{error}} \cdot SS_{error}}$$

where SS_{effect} is the ANOVA sum of squares for the effect of a specific variable, SS_{error} is the sum of squares of the errors after accounting for all experimental variables, df_{effect} and df_{error} are the degrees of freedom for the variable and the error respectively and N is the number of observations (number of trials x number of time bins). $SS_{effect\ x\ time}$ is the ANOVA type II sum of squares for the interaction of a specific variable (i.e., target direction) with time, and $df_{effect\ x\ time}$ are the corresponding degrees of freedom. We included the interaction term since it quantifies the time-varying coding of the variable.

Appendix

Let X be the activity of a neuron where the activity is composed of a signal and a noise term:

$$X_i(t) = \overline{X}_i(t) + \varepsilon_i(t)$$

where t is the time on a trial, $\overline{X}_i(t)$ is the average activity in a task condition i and corresponds to the signal term, and $\varepsilon_i(t)$ is the noise term. We assume the following assumptions regarding the distribution of the noise term:

(1) Zero average; i.e., $\overline{\varepsilon_i(t)} = 0$, for all t.
(2) Is uncorrelated with the signal across time; i.e., $COV(\overline{X}_i(t), \varepsilon_i(t)) = 0$.
(3) Noise terms across different task conditions are uncorrelated; i.e., $COV(\varepsilon_i(t), \varepsilon_j(t)) = 0$
(4) Noise is drawn independently across trials.

The calculations below are always performed over time, so for brevity, we omit the t in the equations.

Since noise and signal are uncorrelated and noise is drawn independently across trials, the covariance between activity in two trials from two task conditions is equal to the covariance of the average activity:

$$COV(X_i, X_j) = COV(\overline{X}_i + \varepsilon_i, \overline{X}_j + \varepsilon_j) = COV(\overline{X}_i, \overline{X}_j) + COV(\overline{X}_i, \varepsilon_j) + COV(\overline{X}_j, \varepsilon_i) + COV(\varepsilon_i, \varepsilon_j) = COV(\overline{X}_i, \overline{X}_j)$$

The correlation coefficient between two trials is defined as:

$$r_{i,j} \triangleq \frac{COV(X_i, X_j)}{\sqrt{\mathcal{V}ar[X_i]} \cdot \sqrt{\mathcal{V}ar[X_j]}} = \frac{COV(\overline{X}_i, \overline{X}_j)}{\sqrt{\mathcal{V}ar[X_i]} \cdot \sqrt{\mathcal{V}ar[X_j]}}$$

where i and j correspond to two task conditions.

The *Between* score is the correlation coefficient for trials in which $i \neq j$.
When calculating $r_{i,j}$ for different trials in the same condition ($i = j$) it can be written as:

$$r_{i,i} = \frac{COV(\overline{X}_i, \overline{X}_i)}{\sqrt{\mathcal{V}ar[\overline{X}_i]} \cdot \sqrt{\mathcal{V}ar[\overline{X}_i]}} = \frac{\mathcal{V}ar[\overline{X}_i]}{\mathcal{V}ar[\overline{X}_i]}$$

The *Within* score is defined as:

$$Within_{i,j} = \sqrt{r_{i,i} \cdot r_{j,j}} = \frac{\sqrt{\mathcal{V}ar[\overline{X}_i] \cdot \mathcal{V}ar[\overline{X}_j]}}{\sqrt{\mathcal{V}ar[X_i] \cdot \mathcal{V}ar[X_j]}}$$

Therefore, the ratio between scores is:

$$\frac{Between_{i,j}}{Within_{i,j}} = \frac{\frac{COV(\overline{X}_i, \overline{X}_j)}{\sqrt{\mathcal{V}ar[\overline{X}_i]} \cdot \sqrt{\mathcal{V}ar[\overline{X}_j]}}}{\frac{\sqrt{\mathcal{V}ar[\overline{X}_i] \cdot \mathcal{V}ar[\overline{X}_j]}}{\sqrt{\mathcal{V}ar[X_i] \cdot \mathcal{V}ar[X_j]}}} = \frac{COV(\overline{X}_i, \overline{X}_j)}{\sqrt{\mathcal{V}ar[\overline{X}_i] \cdot \mathcal{V}ar[\overline{X}_j]}}$$

This means that the ratio of the *Between* to the *Within* scores is equal to the correlation coefficient between the signal (average response) of the activity in the two task conditions. Note that when at least one of the neurons does not respond, the ratio is not defined since $\mathcal{V}ar[\overline{X}_i] = 0$. In practice, these conditions are identified as neurons with small within and between scores (e.g., green dots in Figure 2D). In this regime, trial-by-trial variability cannot be dissociated from the signal and is considered to be inconclusive with respect to the diversity of the responses.

For each pair of trial conditions, we estimated the within and between scores by averaging their values across all possible pairs of trials, excluding the correlation of a trial with itself.